International Journal of General Medicine

Dovepress
Taylor & Francis Group

Open Access Full Text Article

ORIGINAL RESEARCH

RCN1 Binds KIF14 and Promotes the Malignant Growth of Cervical Cancer Through the PI3K-AKT Pathway

Yanyu Li[1–4,*], Li Cai[2,3,*], Jiayun Zhou[2–4,*], Xuping Zhang[2–4], Yunuo Zheng[2–4], Jingbo Zhang[2–4], Hui Cheng[2–4], Qing Wang[2–4], Bei Zhang[1–4]

[1]Suzhou Medical College of Soochow University, Suzhou, Jiangsu, People's Republic of China; [2]Department of Gynecology and Obstetrics, Xuzhou Central Hospital, Xuzhou, Jiangsu, People's Republic of China; [3]Department of Gynecology and Obstetrics, Xuzhou Clinical School of Xuzhou Medical University, Xuzhou, Jiangsu, People's Republic of China; [4]Department of Gynecology and Obstetrics, Xuzhou Central Hospital Affiliated to Southeast University, Xuzhou, Jiangsu, People's Republic of China

*These authors contributed equally to this work

Correspondence: Bei Zhang; Qing Wang, Email bettyzhang10@163.com; qingzi4310513@126.com

Purpose: The fourth most common cause of cancer-related deaths in women is cervical cancer. Though treatment of early-stage cervical cancer is often effective, middle and advanced stage cervical cancer is hard to treat and prone to recurrence. We sought to explore the mechanism underlying cervical cancer progression to identify new therapeutic approaches.

Methods: Label-free mass spectrometry (LC-MS/MS) was used to identify differentially expressed proteins in cervical cancer and normal tissues. The findings were confirmed by Western blotting, RT-qPCR, and immunohistochemistry. The function of RCN1 in tumor invasion, metastasis, and proliferation was investigated using in vitro and in vivo tests. Immunoprecipitation tandem mass spectrometry (IP-MS) was performed in RCNI knockdown cells to identify downstream pathways. Western blotting was used for detecting the expressions of the key proteins included in KIF14 and PI3K-AKT-mTOR signaling pathways before and after RCN1 knockout.

Results: RCN1 expression is elevated in patients with lymph node metastases and recurrent cervical cancer and correlates with poor prognosis. Knockdown and overexpression assays revealed that RCN1 promotes proliferation, migration and invasion of cervical cancer cells. RCN1 overexpression encourages metastasis in a mouse xenograft model. Furthermore, RCN1 targets KIF14, an activator of AKT, thus providing a molecular basis that could explain the malignant behavior of RCN1-expressing cervical cancer.

Conclusion: RCN1 is significantly expressed in cervical cancer, which is associated with a poor prognosis, spread and recurrence. By promoting KIF14-induced activation of the PI3K-AKT-mTOR pathway, RCN1 may facilitate the malignant development of cervical cancer.

Keywords: RCN1, KIF14, cervical cancer, PI3K-AKT-mTOR pathway, label-free mass spectrometry

Introduction

In women, cervical cancer ranks fourth in terms of cancer diagnoses, and fourth in terms of cancer-related deaths. There were 342,000 estimated cancer-related fatalities worldwide in 2020, along with 604,000 new instances of cervical cancer.[1] In some industrialized nations, cytology testing and HPV vaccination constitutes a successful preventative program, although global coverage is still low. Patients with early-stage cervical cancer are now advised to consider surgery or radiation therapy, both of which have good clinical results worldwide.[2,3]

Nevertheless, the most recent version of China's national cancer statistics, published in February 2022 by the National Cancer Center (NCC), showed that the age-standardized incidence rate (ASIR) and age-standardized mortality rate (ASMR) for malignancies of the cervix has increased significantly.[3] This is largely attributed to cancers that are detected in later stages; once cervical cancer metastasis and recurrence occur, the treatments are limited and the prognosis is much worse. The search for more effective molecular targets is therefore of great significance for evaluating the prognosis and treatment of recurrent cervical cancer.

Received: 1 May 2025
Accepted: 26 August 2025
Published: 2 September 2025

Reticulocalbin 1 (RCN1) belongs to the CREC family of compounds. Its carboxyl-terminal sequence contains six EF-hand motifs and an endoplasmic reticulum-retention motif (HDEL) that facilitates its localization to the endoplasmic reticulum. As a Ca^{2+}-binding protein, RCN1 is expressed along the full mammalian cell secretory route and plays a role in regulating Ca^{2+}-dependent processes in the endoplasmic reticulum lumen.[4] Breast cancer,[5] renal cancer,[6] oral cancer,[7] and lung cancer[8] have all been linked to RCN1. Additionally, RCN1 down-regulation has been shown to promote necroptosis and apoptosis in prostate cancer cells.[9] In particular, RCN1 is involved in the regulation of drug resistance. RCN1 knockdown in nasopharyngeal carcinoma cells and tissues decreases doxorubicin resistance and increases cell death.[10] These data suggest that RCN1 dysregulation may play a role in the initiation and spread of malignancies. However, neither the biological actions of RCN1 nor their link to prognosis in cervical cancer have been thoroughly studied.

Kinesins are cargo-carrying molecular motors that travel along microtubules and are ATP-dependent, they are divided into 14 different families, each of which has unique structural and functional traits.[11] Kinesin family member 14 (KIF14) is a chromokinesin that is located on chromosome 1q32.1 and belongs to the Kinesin-3 super family.[12] In hepatocellular carcinoma cells, the loss of KIF14 causes cytokinesis failure and increased amounts of p27 Kip1.[13,14] It is commonly acknowledged that KIF14 contributes to carcinogenesis. When KIF14 is overexpressed, mitosis proceeds quickly and incorrectly, resulting in aneuploidy during the tumor-forming process.[15] Akt also has been implicated in cell division and metastasis and is known to be activated by KIF14.[16] Moreover, suppression of KIF14 impaires AKT activation and hampered cytokinesis to inhibit hepatocellular carcinoma cell growth, and reverses sorafenib resistance.[17] PI3K-AKT has been confirmed to promote the development of tumors; however, it has not been determined whether RCN1 targets KIF14 to activate the PI3K-AKT signaling pathway in cervical cancer.

In this study, we demonstrated that RCN1 is upregulated in cervical carcinoma. To better understand RCN1's potential mode of action, we examined the correlation of RCN1 expression with prognosis and survival. In addition, cellular and animal experiments were conducted to investigate whether RCN1 regulates the mechanism by which PI3K-AKT signaling cathartic promotes malignant behavior via targeting KIF14. Our results provide a new biomarker and potential therapeutic target for advanced cervical cancer.

Materials and Methods

Patient Enrollment

Cervical squamous cell carcinoma tissue, cervical adenocarcinoma tissue, and normal cervical control tissue (patients with hysterectomy due to uterine myoma and no cervical disease confirmed by pathology) specimens were collected by gynecological surgical resection at Xuzhou Central Hospital from 2021 to 2023. There were 44 cases of squamous cell carcinoma, 20 cases of adenocarcinoma, and 60 cases of normal cervical tissue. Additionally, Between January 2016 and July 2018, the Department of Gynecology at Xuzhou Central Hospital collected samples and data from 64 patients who were diagnosed with cervical cancer and had radical surgery. Fresh tissue was frozen in liquid nitrogen immediately after removal, formalin fixed and embedded. All samples used in this study were confirmed pathologically. All patients provided written informed consent prior to sample collection, and the Xuzhou Central Hospital's Ethical Committee approved the use of the clinical samples (XZXY-LJ-20210513-052).

Label-Free Relative Quantification Proteomics

Label-free MS proteomics quantitation (LC-MS/MS) was performed on three groups of samples: cervical adenocarcinoma tissues, cervical squamous carcinoma tissues and normal control tissues, to detect and analyze the significantly differentially expressed proteins in each group of samples. Maxquant Perseus software was used to analyze the differential expression of omics data. The data were imported to retrieve the output proteinGroups.txt file, and the corresponding LFQ intensity was selected. The data with Reverse, only identified by site and < s:1> were removed, the LFQ intensity value was taken as the log base of 2, the disease and control groups were classified, and the effective data were screened. Significant differentially expressed genes (up 2-fold or down 0.5-fold Foldchange (FC), $p < 0.05$) were screened by *t*-test between the two groups. Proteins with pp-regulated or both down-regulated expression in adenocarcinoma (Adeno) and squamous carcinoma (Squa) tissues were analyzed using the InteractiVenn online analysis tool and presented in Venn diagrams. KEGG functional

enrichment analysis was performed to identify differentially expressed proteins. The analyses of up-regulation and down-regulation were conducted separately and together. KEGG pathway enrichment analysis of differentially expressed genes was performed using DAVID 6.8 (or KOBAS) tool, and $p < 0.05$ was selected as the significant threshold. KEGG mapper was used for pathway map analysis of differentially expressed genes.

Cell Culture

The Hela, SiHa, and C33A human cervical cancer cell lines were acquired from Shanghai Gaining Biological Technology Co., Ltd. (Shanghai, China). All cell lines underwent Short Tandem Repeat (STR) profiling authentication. The cells were cultivated in Dulbecco's Modified Eagle's Medium (GIBCO, Billings, MT, United States) supplemented with 10% fetal bovine serum (GIBCO) and 100 IU/mL penicillin-streptomycin combination (Sigma-Aldrich). Cultures of transfected cells were maintained in high-glucose Dulbecco's modified Eagle's medium (GIBCO, USA) supplemented with 10% FBS, 100 U/mL penicillin sodium, and 100 μg/mL streptomycin sulphate (Hyclone, USA). The cells were cultured in a humidified incubator with 5% CO_2 at 37°C.

Immunohistochemistry (IHC)

RCN1 was investigated by IHC in cervical cancer tissues that were fixed in formalin and paraformaldehyde. PowerVisionTM Two-Step Histostaining Reagent (Zhongshan Golden Bridge Biotechnology, Beijing, China) was used for IHC staining. Cytoplasmic staining was independently evaluated by two pathologists in a double-blind fashion. Scores were assigned to the cytoplasm staining intensity (SI) as follows: 0 for negative, 1 for weak, 2 for moderate, or 3 for strong staining. Additionally, scores were assigned for the proportion (PP) of stained cells as follows: 0 (less than 5%), 1 (6–25%), 2 (26–50%), 3 (51–75%), and 4 (more than 75%). Finally, the histoscore (Q) was determined using the following formula: $Q = SI \times PP$. For pathology evaluation, an immunoreactivity score (IRS) of 1–6 was considered low expression of RCN1, while IRS 8–12 was considered strong expression of RCN1.

Real-Time Quantitative PCR (RT-qPCR)

Total RNA was extracted from cervical cancer tissues or cell lines and reverse transcribed into cDNA. Then, RCN1 mRNA expression was assessed by RT-qPCR. The primer sequences were as follows:

RCN1 FORWARD primer GGGAGGAGTTCACTGCCTTTCTG
RCN1 REVERSE primer TCATCCTGATCCACAAACCCATCC
GAPDH FORWARD primer CAGGAGGCATTGCTGATGAT
GAPDH REVERSE primer GAAGGCTGGGGCTCATTT

Western Blot Assay

As directed by the manufacturer, fresh tissues and cell extracts were generated using cell lysis reagent (Sigma-Aldrich, St. Louis, MO, USA), and the protein was measured using a BCA assay (P0010, Biyuntian Institute of Biotechnology, China). Equivalent amounts of protein were separated by 10% sodium dodecyl sulfate-polyacrylamide gel electrophoresis and then detected using rabbit monoclonal antibodies. Among them, anti-RCN1 antibody (P0023D) was from the Biyuntian Institute of Biotechnology in China, anti-KIF14 antibody (DF15723), anti-p-PI3K antibody (AF3242), anti-PI3K antibody (AF6241), anti-p-AKT-antibody (AF0016), anti-AKT antibody (AF6261), anti-p-mTOR antibody (AF3308), and anti-mTOR antibody (AF6308) were all from Affinity Biosciences in China. GAPDH was evaluated as a loading control. Experiments were performed in triplicate.

Vectors Construction and Transfection

GeneChem Corporation (Shanghai, China) designed and constructed lentiviral particles harboring shRNA targeting RCN1 (sh-RCN1) and negative control shRNA (sh-NC). One day before transfection, the C33A or Hela cells were plated in six-well plates. The cells were transfected with the lentiviruses for 12 hours, and then they were selected in puromycin for seven days. Western blotting was used to validate RCN-1 overexpression and knockdown.

Cell Counting Kit 8 (CCK-8) Assay

To determine cell viability, the Cell Counting Kit 8 (TAOSHU, Japan) was utilized. Rapidly proliferating cells were seeded onto 96-well plates, and the optical density at 450 nm was measured using the Gen5 system (BioTek, Winooski, VT, USA) once every 24 hours for three days.

Scratch Tests

Control and RCN1 overexpression cells were seeded at the same concentration (5×10^5 cells/well) in 6-well cell culture plates. After 24 h, a straight line was made perpendicularly in each well using a 200 μL lance tip. Serum-free medium was then added, and the plates were cultured an incubator with 5% CO_2 at 37°C. The cell migration distance was measured under a light microscope at 0 and 24 hours.

Transwell Assays

Transwell invasion assays were conducted using Transwell inserts (Corning, MA, USA) in 24-well plates, with pre-coated Matrigel. Three thousand cells per well were seeded in the top chamber in 200 μL of 2% FBS and 500 μL of 20%. The medium in the lower chamber was supplemented with FBS. After a full day, the lower surface was fixed with methanol and stained with hematoxylin and eosin (H&E), while the upper surface was carefully removed using a cotton swab. Four fields of vision that were chosen at random were measured under a microscope.

IP-MS

C33A sh-RNA cell lines were detected and quantitatively analyzed by mass spectrometry, and the FLQ Intensity (relative quantitative signal values) was evaluated by T-testing. The FLQ Intensity Ratios in samples with p value <0.05 were used as screening criteria to identify and screen highly possible interacting proteins.

Beads were washed three times by adding 500 μL TBS, vortexing, centrifuging for 30s at 5000 g and removing the supernatant. Beads were digested in 100 μL of Buffer 1 (containing 2 M urea, 50 mM Tris-HCl pH 7.5 and 5 μg/mL Trypsin) for 30 m 27°C in a thermomixer, shaking at 800 rpm. After the initial digestion, the samples were centrifuged for 30s at 7000 rpm, and the supernatant was removed and collected into fresh buffer. The beads were washed twice in 50 μL of buffer 2 (containing 2 M urea, 50 mM Tris-HCl pH 7.5 and 1 mM DTT), and the supernatants were pooled. The samples were left on the bench to continue digesting overnight at room temperature. Then, the samples were treated with 1 μL trifluoroacetic acid (TFA) to stop the digestion and were desalted in C18 stagetips. Tryptic peptides were desalted and centrifuged in a speedvac to dry. Then, Tryptic peptides were dissolved in 0.1% FA.

Liquid Chromatography–Tandem Mass Spectrometry (LC–MS/MS)

For LC-MS/MS analysis, the peptides were separated by a 60 min gradient elution at a flow rate of 0.22 μL/min with a Thermo Scientific EASY-nLC 1000 HPLC system, which was directly interfaced with a Thermo Scientific Orbitrap Exploris 480 mass spectrometer that was operated in the data-dependent acquisition mode using Xcalibur 3.0 software. This included a single full-scan mass spectrum in the orbitrap (300–2000 m/z, 70,000 resolution) followed by 20 data-dependent MS/MS scans at 27% normalized collision energy (HCD).

MS/MS spectra from raw data were imported to Proteome Discoverer (version 3.0, Thermo Scientific), and a database search was performed using MS CHIMERYS™ with a combination of human proteins (uniprot reference, version 2022–02-03, 20,509 entries) as well as common contaminants (PD_Contaminants, 344 entries). The intensity from PD was further processed in the Perseus computational platform (v 1.6.7.0). LFQ intensity values were log2 transformed, and the samples were grouped into experimental categories. Proteins not identified in 3 out of 3 replicates in at least one group were also removed. Missing values were imputed using normally distributed values with a 1.8 downshift (log2) and randomized 0.3 width (log2) for whole matrix values. Statistical analysis was performed to determine which proteins were significantly enriched in the C33A cell compared to the C93 cell samples or isotype IgG control sample (*t*-test with permutation-based False Discovery Rate (FDR) = 0.05 and S0 = 0.1).

In vivo Assays

Two sets of female NKG mice were utilized to monitor tumor growth: oe-C33A-NC [mice implanted with control C33A cells (n = 8) that were infected with scrambled oeRNA]; and oe-C33A-RCN1 [mice inoculated with RCN1 oeRNA-infected C33A cells (n = 8)]. The mice were subcutaneously injected with 5×10^6 cells/100 μL. Every three days, the longest and shortest diameters of the developing tumors were measured using calipers, and the tumor volume (V) was calculated using the formula: V = (the longest diameter the shortest diameter2)/2. Cervical cancer metastasis was determined using a model of pulmonary metastasis. Live imaging was conducted once every 3 days, and the mice were euthanized 1 month after injection.

Statistical Analysis

Categorical variables were quantified with n (%), whereas continuous variables were calculated using the meanSD of at least three independent experiments. Data analysis and chart drawing were performed using GraphPad Prism 6.0. Independent sample *t* test was used for data comparison between the two groups, and one-way analysis of variance was used for multi-group comparison, p value <0.05 was considered statistically significant.

Results

Identification of Differentially Expressed Proteins by Proteomic and Bioinformatics Methods

To evaluate differentially expressed proteins in cervical cancer, we performed label-free mass spectrometry (LC-MS/MS) of 12 paired cervical cancer cases (including 6 squamous cell carcinomas and 6 adenocarcinomas) and 6 normal tissue samples. A total of 547 up-regulated genes and 222 down-regulated genes were differentially expressed in both squamous cell carcinoma and adenocarcinoma (Figure 1A). Heat maps of the top 20 elevated and decreased proteins are shown (Figure 1B). Notably, this includes RCN1, a Ca2+-binding protein that has been shown to be overexpressed in a variety of other cancer types. According to KEGG function enrichment analysis, "protein processing in endoplasmic reticulum" was the primary pathway that was differentially regulated in cervical cancer (Figure 1C). Given that RCN1 resides in the endoplasmic reticulum, these results are consistent with the possibility that RCN1 expression may contribute to cervical cancer.

RCN1 is Highly Expressed in Cervical Cancer

To verify the elevated expression of RCN1 in cervical cancer, we assessed the degree of RCN1 expression in 64 cervical cancer samples and 60 nontumor tissues by immunohistochemistry (IHC) analysis. The results revealed that RCN1 is highly expressed in both squamous carcinoma and adenocarcinoma as compared to normal cervix tissues (Figure 2A). These findings were confirmed by RT-qPCR and Western blot analyses (Figure 2B and C). Furthermore, RCN1 was expressed at higher levels in cervical cancer cell lines (C33A and Hela) as compared to normal cervical epithelial cells (N) (Figure 2D). These results confirm the elevated expression of RCN1 in cervical cancer.

Poor Prognosis is Indicated by High Expression of RCN1 in Cervical Cancer

To further elucidate the clinical importance of RCN1 in cervical cancer, we assessed the association between RCN1 expression and clinicopathological features of cervical cancer using Fisher's exact test. Based on the Immunoreactivity score (IRS) from the IHC assays, we divide the cervical cancer tissue samples into those with high (51.6%, 33/64) and low (48.4%, 31/64) RCN1 expression. A positive association of high RCN1 expression was observed with tumor lymph node metastasis (p = 0.039) and recurrence (p = 0.018); however, a correlation was not observed with age, tumor size, differentiation, FIGO 2018 stage, or pathological tumor type (Table 1).

For additional prognostic verification, we evaluated RCN1 expression according to data in the TCGA database. There was a statistically significant difference in the disease-free survival (Figure 3A) and overall survival (Figure 3B) of patients with cervical cancer who had high vs low expression of RCN1. These results suggest that high RCN1 expression in cervical cancer patients may be a useful prognostic marker for metastasis, recurrence and survival.

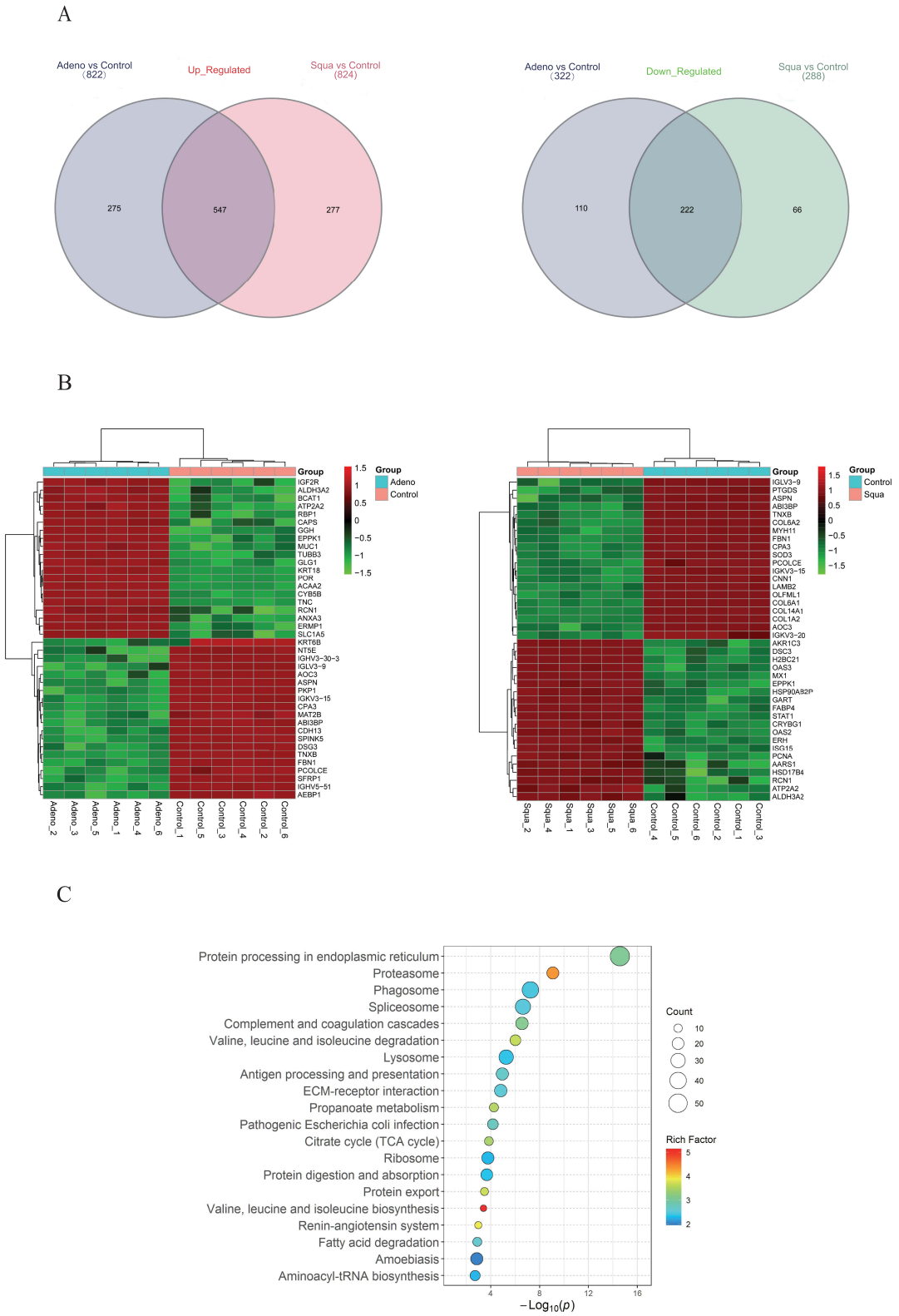

Figure 1 Identification of key proteins in cervical cancer by proteomic and bioinformatics methods. (**A**) Venn diagrams of up-regulated and down-regulated proteins in squamous carcinoma (Squa) and adenocarcinoma (Adeno) tissues. Expression was calculated relative to normal control tissues. (**B**) Heat map of the top 20 differentially expressed proteins in normal cervical tissues, cervical squamous carcinoma tissues, and cervical adenocarcinoma tissues. RCN1 is boxed in red. (**C**) KEGG functional enrichment analysis showed that the differentially expressed proteins are mainly concentrated in the "protein processing in endoplasmic reticulum" pathway.

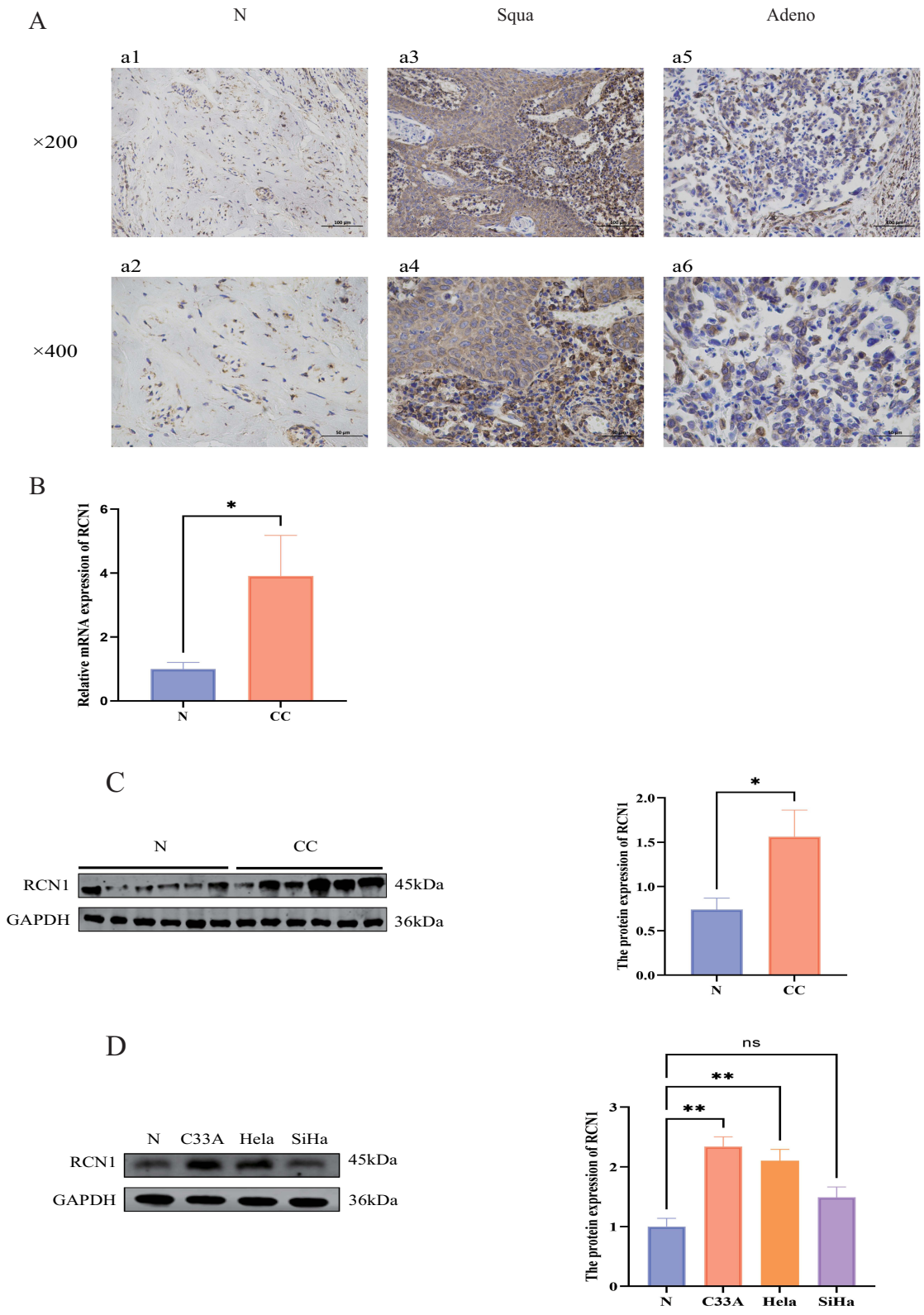

Figure 2 RCN1 is overexpressed in cervical cancer. (**A**) Immunohistochemistry of RCN1 expression in cervical tissues. a1, a2 Expression of RCN1 in normal cervix(N). a3, a4 Expression of RCN1 in squamous carcinoma (Squa). a5, a6 Expression of RCN1 in adenocarcinoma (Adeno). Results are representative of n = 64 samples (SP×200, ×400). (**B**) Expression of RCN1 mRNA in cervical cancer tissues (CC) compared with normal cervix tissues(N) as evaluated by RT-qPCR. (**C**) RCN1 protein expression in cervical cancer tissues compared to the normal cervix tissues(N) as evaluated by Western blotting. (**D**) Western blotting of RCN1 in normal cervical epithelial cells (N) and the cervical cancer cell lines C33A, Hela, and SiHa compared to the Normal group. The data are expressed as mean±SEM, with $*p < 0.05$, $**p < 0.01$, as compared to the normal cervix group. Data marked with "ns" were considered statistically non-significant.

https://doi.org/10.2147/IJGM.S531003

Table 1 Associations of RCN1 Expression with Clinicopathological Characteristics in Cervical Cancer

RCN1 Expression				
Features	**Total (n=64)**	**Low (n=31)**	**High (n=33)**	***P*-value**
Age				0.817
≤50	29	16	13	
>50	35	15	20	
Tumor size				0.697
<4cm	42	19	23	
≥4cm	22	12	10	
Differentiation				0.560
Highly and moderately	47	22	25	
Lowly	17	9	8	
Lymphatic metastasis				0.039*
No	57	29	28	
Yes	7	2	5	
FIGO stage				0.671
I	41	29	12	
II–III	23	10	13	
Recurrence				0.018*
Yes	8	2	6	
No	56	29	27	
Pathological				0.561
Squamous carcinoma	44	24	20	
Adenocarcinoma	20	7	13	

Note: *$p<0.05$.

RCN1 Promotes Cervical Cancer Cell Invasion, Migration, and Proliferation

To investigate the role of RCN1 in cervical cancer, we knocked down RCN1 in C33A and Hela cervical cancer cells (Figure 4A and B). Cell counting kit-8 (CCK8) assays demonstrated that RCN1 knockdown inhibited cervical cancer cell proliferation. (Figure 4C and D). Furthermore, RCN1 knockdown decreased the migratory and invasive characteristics of cervical cells, as indicated by Transwell and cell wound scratch assays (Figure 4E–H).

For additional verification, we overexpressed RCN1 in C33A and Hela cells (Figure 5A and B). CCK-8 assays demonstrated that RCN1 overexpression promotes cervical cancer cell proliferation (Figure 5C and D). Furthermore, scratch tests and Transwell assays revealed that RCN1 overexpression markedly increases migration and invasion. (Figure 5E–H). These findings confirm that RCN1 expression promotes cervical cancer cell growth and metastasis.

RCN1 Binds KIF14 in Cervical Cancer Cells

To further investigate proteins that interact with RCN1 in cervical cancer cells, we performed immunoprecipitation tandem mass spectrometry (IP-MS) quantitative difference comparison. A total of 345 proteins were significantly enriched and bound to RCN1 in shRCN1 vs shNC C33A cells (Figure 6A); and 100 proteins were significantly enriched in the RCN1 antibody vs IgG group (Figure 6B). At the intersection, 20 proteins with RCN1 binding specificity were identified (Figure 6C). This includes, KIF14, a downstream protein of RCN1 that promotes phosphorylation of AKT, leading to malignant behavior of cervical cancer.

RCN1 Regulates the PI3K-AKT Signaling Pathway by Targeting KIF14

To detect whether RCN1 regulates the PI3K/AKT/mTOR signaling pathway by targeting KIF14 in cervical cancer, RCN1 were knocked-down and overexpressed individually in cervical cancer cells (C33A and Hela) using lentivirus. The

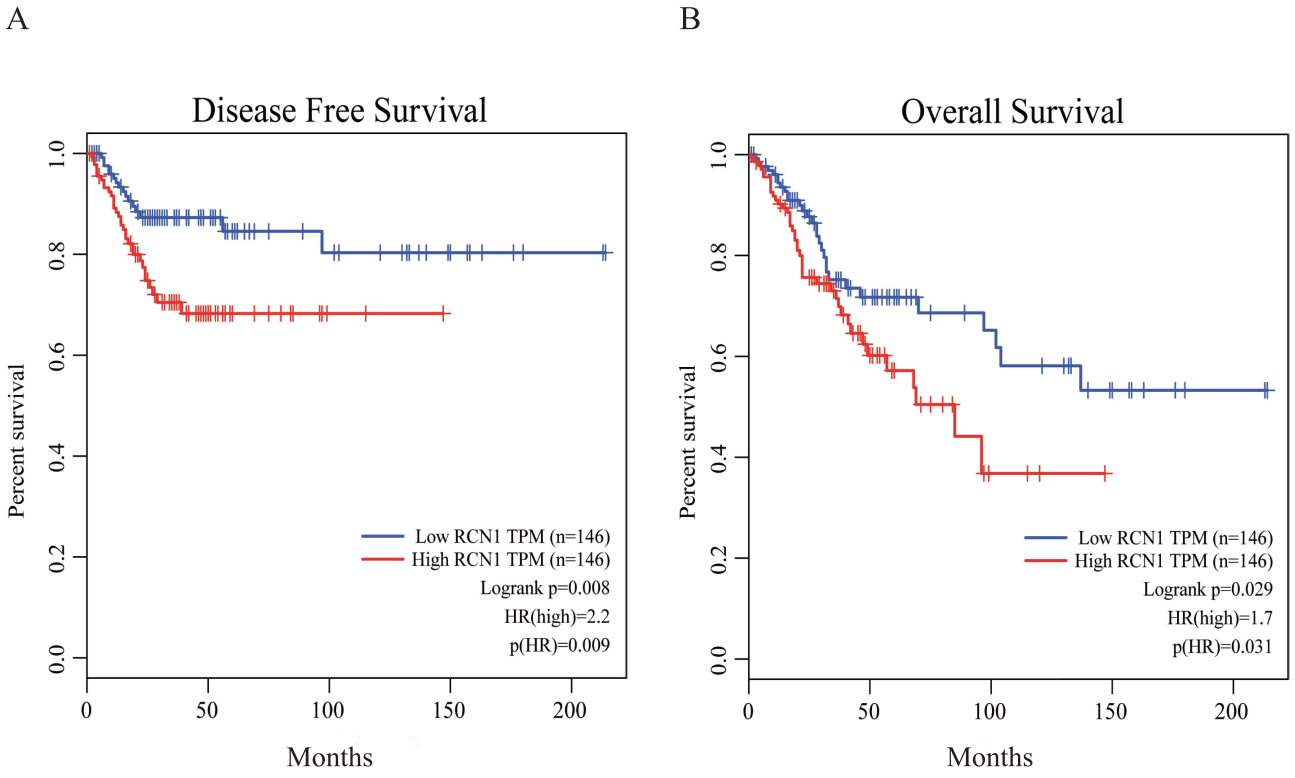

Figure 3 RCN1 expression correlates with survival. Kaplan-Meier analysis of RCN1 expression. Patients with cervical cancer who expressed high levels of RCN1 in the TCGA database showed a shorter disease-free survival time (**A**) and a shorter overall survival time (**B**) ($p < 0.05$) than patients who expressed low levels of RCN1.

expressions of KIF14 and PI3K/AKT/mTOR signaling pathway proteins were detected by Western blotting. The results showed that the levels of KIF14, p-PI3K, p-AKT, and p-mTOR were reduced with the downregulation of RCN1, and increased with the upregulation of RCN1 (Figure 7A and B), which indicated that RCN1 activates the PI3K/AKT/mTOR signaling pathway by targeting KIF14, and promotes the malignant behavior of cervical cancer cells.

RCN1 Promotes Cervical Cancer Cell Growth and Metastasis in vivo

To determine whether RCN1 expression regulates cervical cancer progression in vivo, we generated a cervical cancer model using female NKG mice injected with control C33A cells or C33A cells overexpressing RCN1. The group with upregulated RCN1 had a higher average tumor volume and more metastasis (Figure 8A and B). These results confirm that RCN1 promotes cervical cancer growth and metastasis in vivo.

Discussion

Despite the availability of protective vaccines, cervical cancer is one of the most significant gynecological issues. Its high incidence and death rate largely are attributed to countries with low and medium incomes.[18] China and India account for over a third of the cervical burden worldwide, with 106 000 cases and 48 000 deaths in China and 97 000 cases and 60 000 deaths in India each year. Most cervical cancer patients who receive contemporary treatment are cured; however, 13% of individuals with cervical cancer receive a diagnosis at an advanced stage. For metastatic cervical cancer, the 5-year survival rate is only 16.5%.[19] Even with pelvic dissection, the 5-year survival rate for individuals with R1 resection following recurrent cervical cancer is close to zero.[20,21] Because of the poor prognosis and lack of available therapeutic options, recurrent cervical cancer remains a significant challenge. Therefore, finding reliable molecular indicators of cervical cancer malignancy is crucial.

In this study, we detected the proteins in clinically collected cervical cancer specimens using LC-MS/MS technology and conducted differential protein screening using bioinformatics approaches. In KEGG functional enrichment analysis, "protein

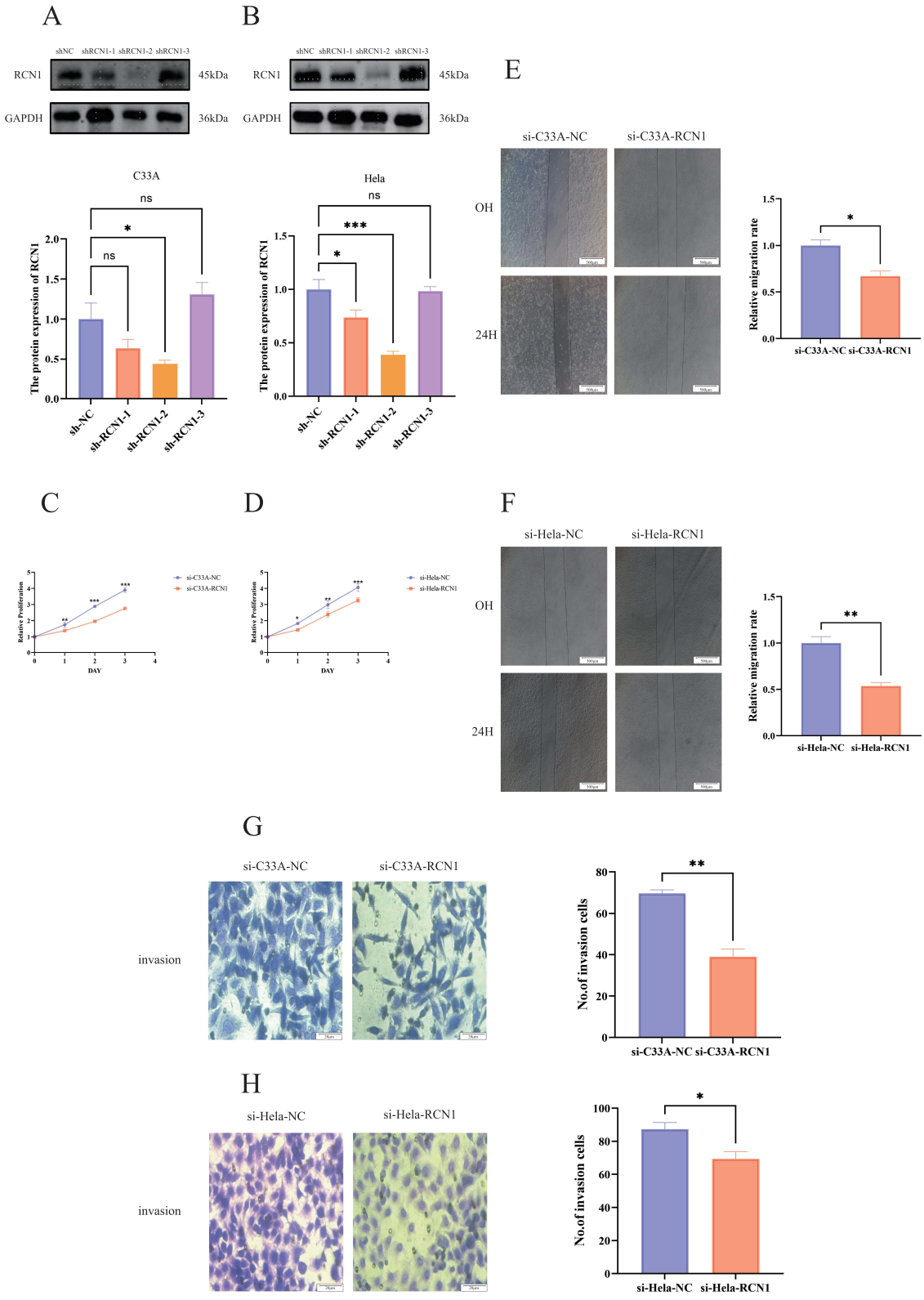

Figure 4 RCN1 knockdown suppresses cell proliferation, migration and invasion of cervical cancer cells. (**A**) Construction of RCN1 knockdown C33A cells. (**B**) Construction of RCN1 knockdown Hela cells. (**C**) CCK-8 assay of cell growth in control and RCN1 knockdown C33A cells. (**D**) CCK-8 assay of cell growth in control and RCN1 knockdown Hela cells. (**E**) Scratch test assay of the impact of RCN1 knockdown on the migration of C33A cells. (**F**) Scratch test assay of the impact of RCN1 knockdown on the migration of HeLa cells. (**G**) Transwell assay of the impact of RCN1 knockdown on the invasiveness of C33A cells. (**H**) Transwell assay of the impact of RCN1 knockdown on the invasiveness of Hela cells. The data are shown as mean±SEM for n = 3. *$p < 0.05$, **$p < 0.01$, ***$p < 0.001$, as compared to the NC group. Data marked with "ns" were considered statistically non-significant.

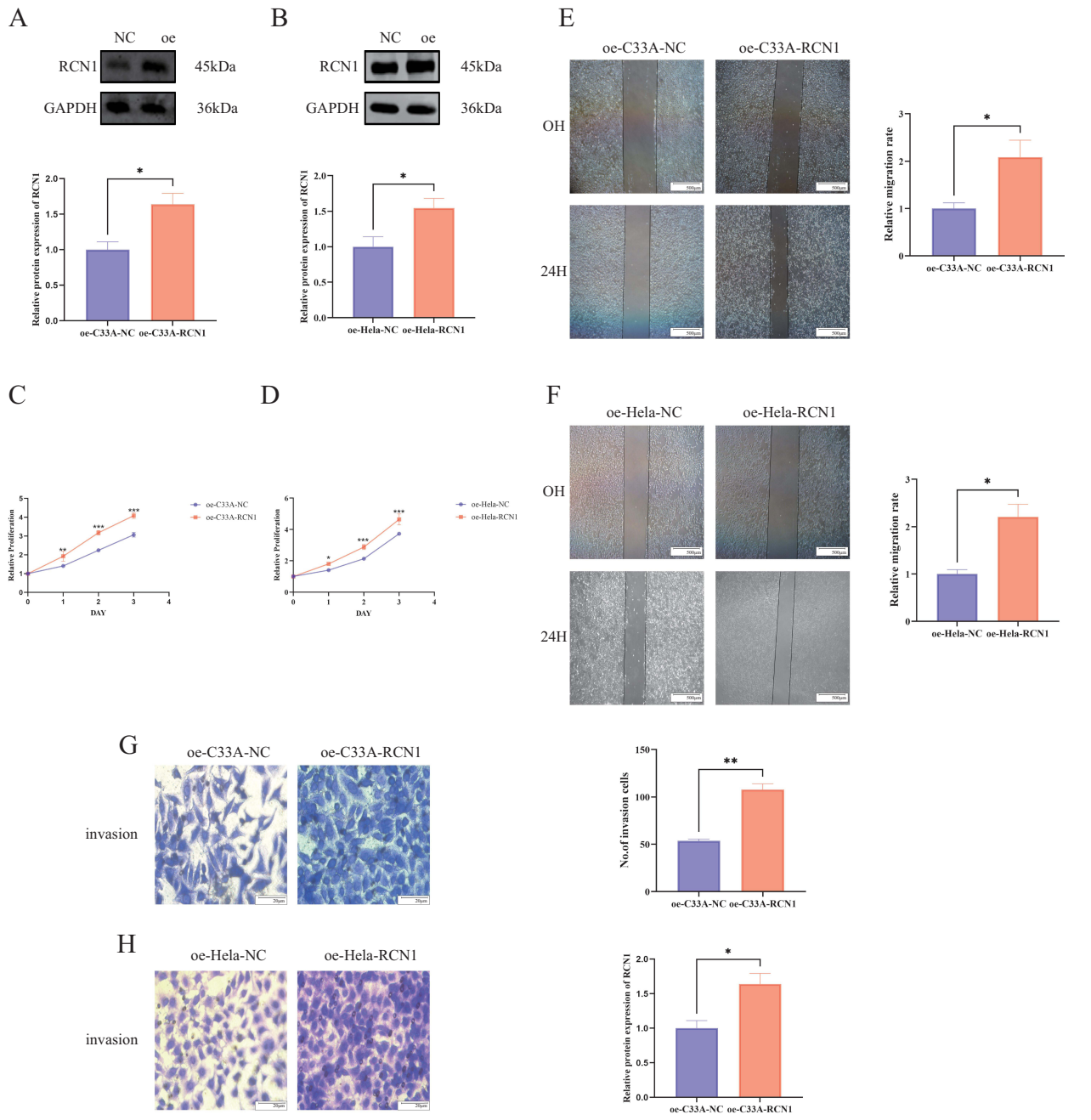

Figure 5 Overexpression of RCN1 stimulates cervical cancer cell motility, invasion, and proliferation. (**A**) Construction of RCN1 overexpression C33A cells. (**B**) Construction of RCN1 overexpression Hela cells. (**C**) CCK-8 assay of cell growth in control and RCN1 overexpression C33A cells. (**D**) CCK-8 assay of cell growth in control and RCN1 overexpression Hela cells. (**E**) Scratch test assay of the impact of RCN1 overexpression on the migration of C33A cells. (**F**) Scratch test assay of the impact of RCN1 overexpression on the migration of HeLa cells. (**G**) Transwell assay of the impact of RCN1 overexpression on the invasiveness of C33A cells. (**H**) Transwell assay of the impact of RCN1 overexpression on the invasiveness of Hela cells. The data are presented as mean±SEM, n = 3, *$p < 0.05$, **$p < 0.01$, ***$p < 0.001$, as compared to the NC group.

processing endoplasmic reticulum", "proteasome", "phagosome", "spliceosome" and "complement and coagulation cascade" were the top five pathways. The endoplasmic reticulum is linked to several cellular processes, including protein synthesis, transcription, cell maturation, secretion, membrane protein folding, and Ca_2+ homeostasis. Furthermore, the endoplasmic reticulum is a crucial regulator of cell homeostasis.[22,23] Various endogenous or exogenous stimuli, such as hypoxia, nutrient deficiency, and chemotherapy drugs, can interfere with or disrupt endoplasmic reticulum homeostasis, triggering a cell state called "endoplasmic reticulum stress (ERS)." To overcome stress and restore protein stability, ERS activates the unfolded protein response (UPR). This initiates a cascade of subsequent signals to preserve endoplasmic reticulum homeostasis.[24] ERS

https://doi.org/10.2147/IJGM.S531003

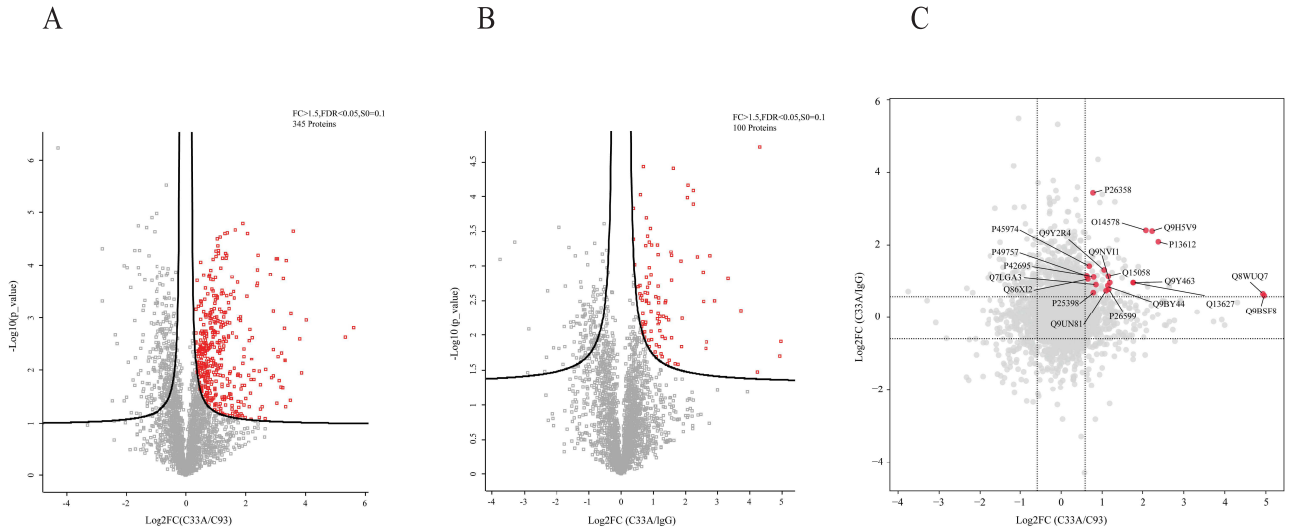

Figure 6 IP-MS of RCN1 binding partners. (**A**) Mass spectrometry quantitative difference comparison of proteins bound to RCN1 in shRCN1 vs shNC C33A cells, Fold change >1.5, FDR < 0.05, S0 = 0.1. (**B**) Mass spectrometry quantitative difference comparison of proteins bound to RCN1 in the RCN1 antibody vs IgG group, Fold change >1.5, FDR < 0.05, S0 = 0.1. (**C**) Pairwise comparison of proteins that differentially bind RCN1 in both shRCN1 vs C33A cells and IgG vs C33A cells. The proteins marked in red in Figures A and B are those significantly enriched in the experimental group compared to the control group. The red proteins in Figure C are those enriched relative to both control groups, the interacting proteins. In all three figures, the gray color indicates proteins that were not significantly enriched.

can be induced by hypoxia, hypoglycemia, chemotherapy drugs or other environmental stimuli during the growth, leading to invasion and metastasis of tumor cells.[25] Tumor cells are considerably less sensitive to chemotherapeutic medications in this stage.[26,27] Therefore, the identification of these KEGG pathways is consistent with a role for ERS in contributing to the poor response to treatment in the advanced stages of cervical cancer.

We also identified the Ca_2+-binding protein RCN1 as a differentially upregulated protein in cervical cancer. RCN1 regulates Ca_2+-dependent activity in the lumen of the endoplasmic reticulum. Our study is the first to evaluate its role in cervical cancer, but prior research on RCN1 has shown that the gene is linked to non-small cell lung cancer, liver cancer, colorectal cancer, and breast cancer. In addition, current studies on the RCN1 pathway focus on ERS and other endoplasmic reticulum-related pathways. These findings are consistent with the possibility that RCN1 may promote the development of cervical cancer through ERS. We confirmed that RCN1 is highly expressed in cervical cancer tissues and cell lines. According to our research, patients with cervical cancer who express high levels of RCN1 have a worse prognosis and a greater likelihood of lymph node metastases. Notably, we demonstrated that RCN1 promotes tumor growth in xenograft mice and is essential for the effective spread of cervical cancer cells to the lung and peritoneal cavity. Our investigation links RCN1 to unfavorable outcomes in cervical cancer patients for the first time, thus providing insight into mechanisms that could lead to new strategies for intervention.

In this study, we also examined potential downstream targets of RCN1 by using IP-MS technology to screen for interacting proteins. Among the putative RCN1 binding partners, KIF14 acts as an oncogene in prostate cancer and has been demonstrated to be a novel and useful predictive biomarker.[28] Studies have shown that KIF14 activates the PI3K/AKT signaling pathway to promote the migration and invasion of bladder cancer.[29] Furthermore, it has been documented that through the activation of Akt, KIF14 has an oncogenic role in glioma/glioblastoma and functions as a potential molecular target and prognostic marker for human gliomas.[30,31] It is well established that activated PI3K/AKT-mTOR signaling promotes invasion, migration, and EMT of tumor cells.[32–36] When overactivity of PI3K occurs and AKT function is obtained, this pathway is overactivated and promotes the development of cancer. IP-MS was used to study the interaction between RCN1 and KIF14. The results suggested that KIF14 may play a role in the PI3K-AKT signaling pathway in various countries. The association was further verified via Western blotting. The results showed that RCNI targeting KIF14 expression affected levels of p-PI3K, p-AKT and p-mTOR. Therefore, our study suggested that KIF14 is activated by RCN1, thereby regulating the PI3K/AKT signaling pathway and promoting cervical cancer progression.

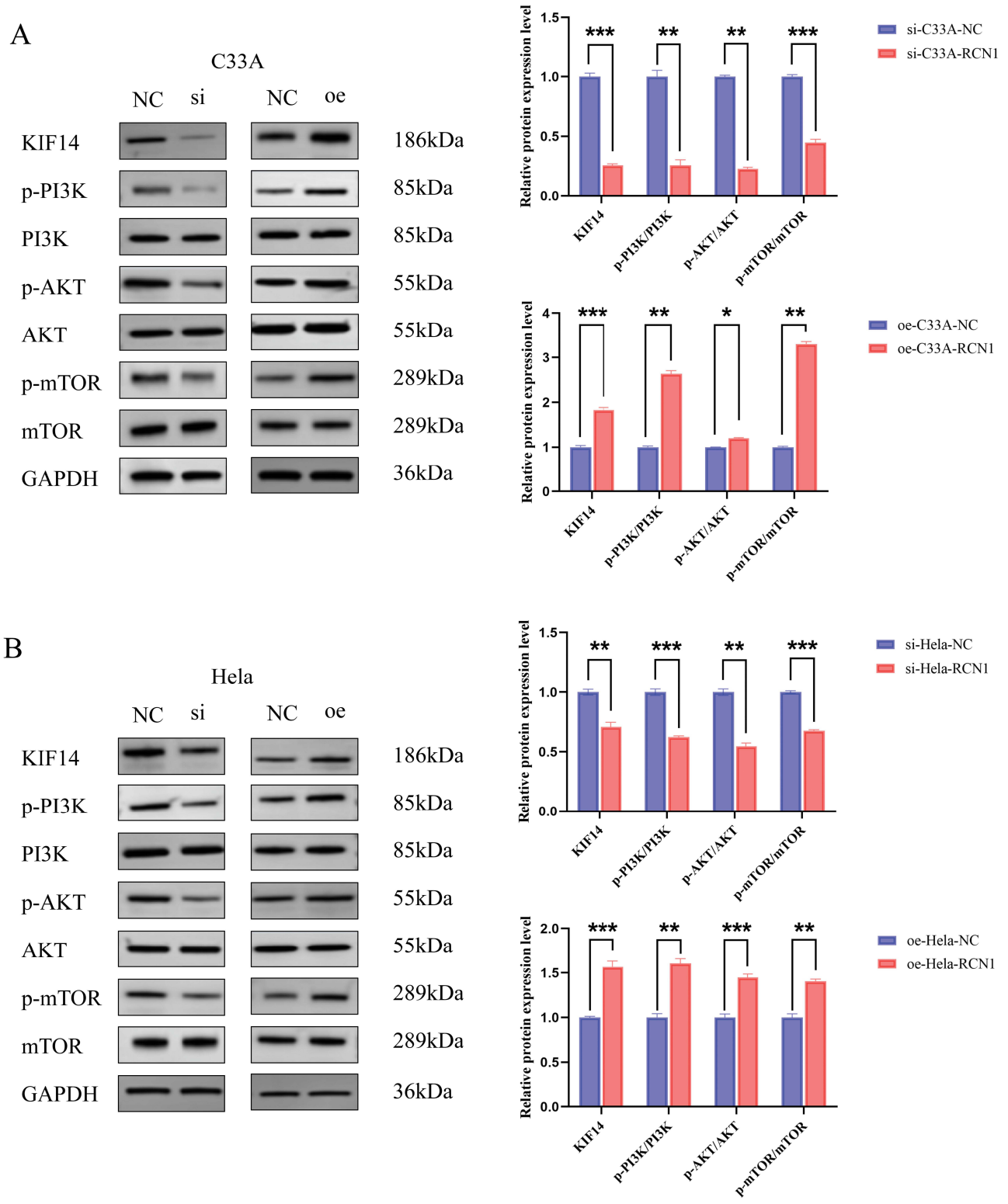

Figure 7 RCN1 regulates the PI3K-AKT signaling pathway by targeting KIF14. (**A**) Effects of RCN1 knockdown and overexpression on key proteins in KIF14, PI3K/AKT/mTOR pathway in C33A cells. (**B**) Effects of RCN1 knockdown and overexpression on key proteins in KIF14, PI3K/AKT/mTOR pathway in Hela cells. The data are shown as mean ± SEM. n = 3. *$p < 0.05$, **$p < 0.01$, ***$p < 0.001$, as compared to the NC group.

https://doi.org/10.2147/IJGM.S531003

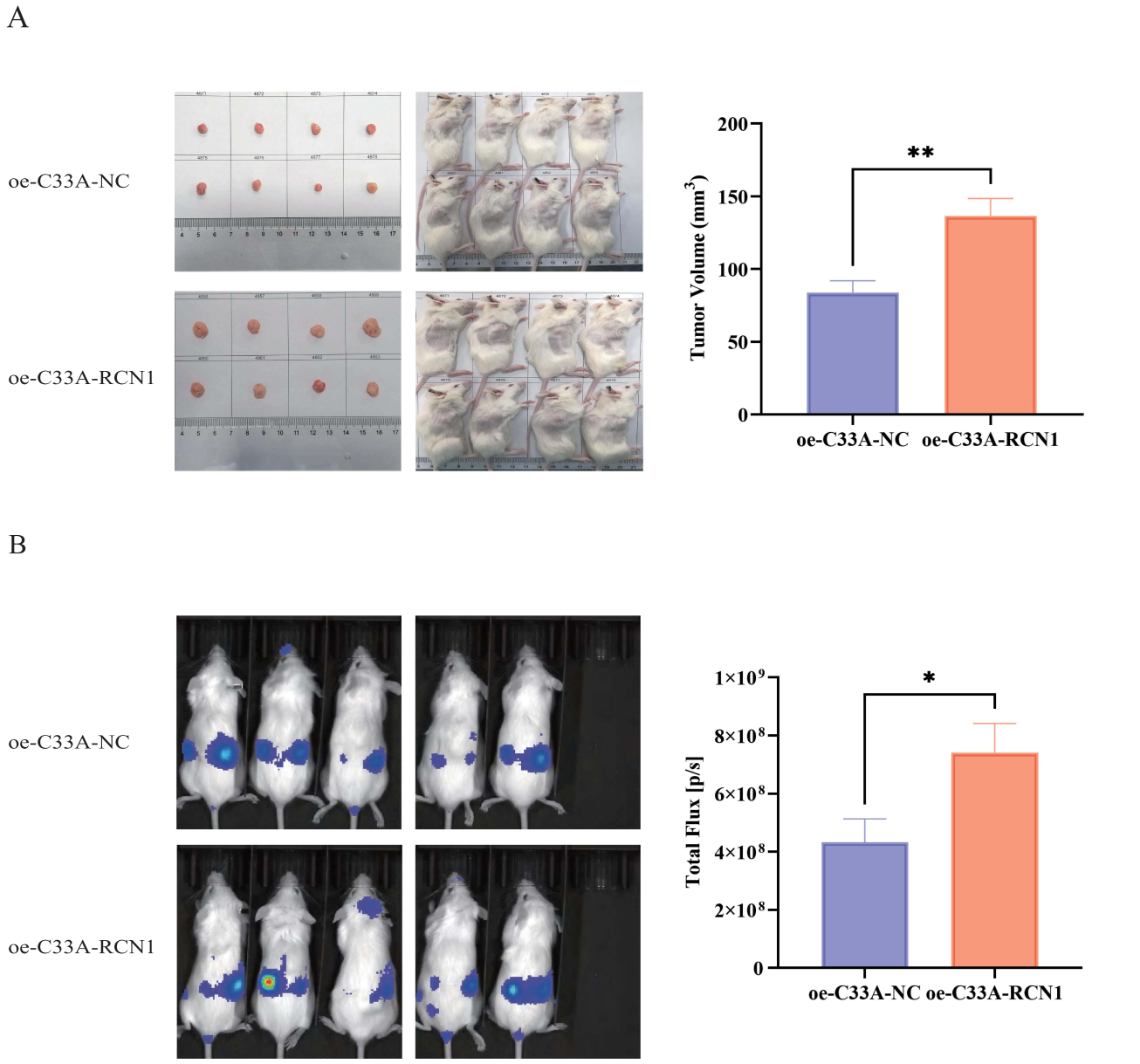

Figure 8 RCN1 promotes metastasis in vivo. (**A**) Final volume of subcutaneous tumors one month after subcutaneous neoplasia. (**B**) Final total flux one month after caudal vein injection. Data are expressed as mean±SEM, n = 6. *$p < 0.05$,**$p < 0.01$, compared with NC group.

In summary, using LC-MS/MS, we discovered that RCN1 is significantly expressed in cervical cancer tissues. The elevated expression level of RCN1 was confirmed in vivo, and additional in vitro and in vivo studies demonstrated its promotion of tumor invasion, growth, and metastasis. Subsequently, IP-MS indicated that RCN1 may target KIF14, which provides a potential mechanism for its involvement in the malignant progression of cervical cancer. Our study suggests that RCN1 targeting KIF14 stimulates the PI3K/AKT signaling pathway and promotes malignant behavior of tumor cells. The findings of this study may pave the way for future investigations into the development of targeted therapies for cervical cancer.

Data Sharing Statement

Proteomic raw data are available via iprox under identifier IPX0011476002. IP-MS data are available via iprox under identifier IPX0011476001.

Ethics Statement

The Animal experiments were approved by the Experimental Animal Ethics Committee of Xuzhou Medical University. Animal procedures followed the ethical principles of the Declaration of Helsinki as applicable to veterinary research, and were approved by the Experimental Animal Ethics Committee of Xuzhou Medical University (Approval No. 202308T032).All patients provided written informed consent prior to sample collection, and the Xuzhou Central Hospital's Ethical Committee approved the use of the clinical samples (XZXY-LJ-20210513-052).

Acknowledgments

Yanyu Li, Li Cai and Jiayun Zhou are regarded as co-first authors for this study. Thank you to the Pathology Department, Imaging Department, and Laboratory for providing auxiliary examination materials for this article, and thank you to the laboratory colleagues for their companionship.

Author Contributions

All authors made a significant contribution to the work reported, whether that is in the conception, study design, execution, acquisition of data, analysis and interpretation, or in all these areas; took part in drafting, revising or critically reviewing the article; gave final approval of the version to be published; have agreed on the journal to which the article has been submitted; and agree to be accountable for all aspects of the work.

Funding

This work was supported by the Xuzhou Medical University affiliated hospital development fund surface project (XYFM202206), Xuzhou Health Commission Special Fund Planning Project (NO. 2019TD005), the Xuzhou science and technology project (KC23181).

Disclosure

The authors declare that the research was conducted in the absence of any commercial or financial relationships that could be construed as a potential conflict of interest.

References

1. Sung H, Ferlay J, Siegel RL, et al. Global cancer statistics 2020: GLOBOCAN estimates of incidence and mortality worldwide for 36 cancers in 185 countries. *CA Cancer J Clin*. 2021;71(3):209–249. doi:10.3322/caac.21660
2. Arbyn M, Weiderpass E, Bruni L, et al. Estimates of incidence and mortality of cervical cancer in 2018: a worldwide analysis. *Lancet Glob Health*. 2020;8(2):e191–e203. doi:10.1016/S2214-109X(19)30482-6
3. Zheng RS, Chen R, Han BF, et al. Cancer incidence and mortality in China, 2022. *Zhonghua Zhong Liu Za Zhi*. 2024;46(3):221–231. doi:10.3760/cma.j.cn112152-20240119-00035
4. Gomez J, Areeb Z, Stuart SF, et al. EGFRvIII promotes cell survival during endoplasmic reticulum stress through a reticulocalbin 1-dependent mechanism. *Cancers*. 2021;13(6):1198. doi:10.3390/cancers13061198
5. Kurpińska A, Suraj J, Bonar E, et al. Proteomic characterization of early lung response to breast cancer metastasis in mice. *Exp Mol Pathol*. 2019;107:129–140. doi:10.1016/j.yexmp.2019.02.001
6. Sun Y, Liu C, Zhong H, Wang C, Xu H, Chen W. Screening of autoantibodies as biomarkers in the serum of renal cancer patients based on human proteome microarray. *Acta Biochim Biophys Sin*. 2022;54(12):1909–1916.DOI:10.3724/abbs.2022189.
7. Liu H, Guo H, Wu Y, et al. RCN1 deficiency inhibits oral squamous cell carcinoma progression and THP-1 macrophage M2 polarization. *Sci Rep*. 2023;13(1):21488. doi:10.1038/s41598-023-48801-2
8. Fu H, Chen R, Wang Y, Xu Y, Xia C, Zhang B. Reticulocalbin 1 is required for proliferation and migration of non-small cell lung cancer cells regulated by osteoblast-conditioned medium. *J Cell Mol Med*. 2021;25(24):11198–11211. doi:10.1111/jcmm.17040
9. Liu X, Zhang N, Wang D, et al. Downregulation of reticulocalbin-1 differentially facilitates apoptosis and necroptosis in human prostate cancer cells. *Cancer Sci*. 2018;109(4):1147–1157. doi:10.1111/cas.13541
10. Huang ZH, Qiao J, Feng YY, et al. Reticulocalbin-1 knockdown increases the sensitivity of cells to Adriamycin in nasopharyngeal carcinoma and promotes endoplasmic reticulum stress-induced cell apoptosis. *Cell Cycle*. 2020;19(13):1576–1589. doi:10.1080/15384101.2020.1733750
11. Benoit M, Asenjo AB, Paydar M, Dhakal S, Kwok BH, Sosa H. Structural basis of mechano-chemical coupling by the mitotic kinesin KIF14. *Nat Commun*. 2021;12(1):3637. doi:10.1038/s41467-021-23581-3
12. Wang H, Tang F, Tang P, Zhang L, Gan Q, Li Y. Noncoding RNAs-mediated overexpression of KIF14 is associated with tumor immune infiltration and unfavorable prognosis in lung adenocarcinoma. *Aging*. 2022;14(19):8013–8031. doi:10.18632/aging.204332
13. Xu H, Choe C, Shin SH, et al. Silencing of KIF14 interferes with cell cycle progression and cytokinesis by blocking the p27(Kip1) ubiquitination pathway in hepatocellular carcinoma. *Exp Mol Med*. 2014;46(5):e97. doi:10.1038/emm.2014.23

14. Cheng C, Wu X, Shen Y, Li Q. KIF14 and KIF23 promote cell proliferation and chemoresistance in HCC cells, and predict worse prognosis of patients with HCC. *Cancer Manag Res*. 2020;12:13241–13257. doi:10.2147/CMAR.S285367
15. Nowosad A, Jeannot P, Callot C, et al. p27 controls Ragulator and mTOR activity in amino acid-deprived cells to regulate the autophagy-lysosomal pathway and coordinate cell cycle and cell growth. *Nat Cell Biol*. 2020;22(9):1076–1090. doi:10.1038/s41556-020-0554-4
16. Manning BD, Cantley LC. AKT/PKB signaling: navigating downstream. *Cell*. 2007;129(7):1261–1274. doi:10.1016/j.cell.2007.06.009
17. Zhu Q, Ren H, Li X, et al. Silencing KIF14 reverses acquired resistance to sorafenib in hepatocellular carcinoma. *Aging (Albany NY)*. 2020;12 (22):22975–23003. doi:10.18632/aging.104028
18. Monk BJ, Enomoto T, Kast WM, et al. Integration of immunotherapy into treatment of cervical cancer: recent data and ongoing trials. *Cancer Treat Rev*. 2022;106:102385. doi:10.1016/j.ctrv.2022.102385
19. Sharma A, Chakdar H, Vaishnav A, et al. Multifarious plant growth-promoting rhizobacterium Enterobacter sp. CM94-mediated systemic tolerance and growth promotion of chickpea (Cicer arietinum L.) under salinity stress. *Front Biosci*. 2023;28(10):241.DOI:10.31083/j.fbl2810241. doi:10.31083/j.fbl2810241
20. Stolnicu S, Hoang L, Soslow RA. Recent advances in invasive adenocarcinoma of the cervix. *Virchows Arch*. 2019;475(5):537–549. doi:10.1007/s00428-019-02601-0
21. Gao X, Kong Y, Ning Y, et al. The prognosis of patients with locally advanced cervical cancer undergoing surgical versus non-surgical treatment: a retrospective cohort study based on SEER database and a single-center data. *Int J Surg*. 2024;111(1):1619–23.DOI:10.1097/JS9.0000000000002098.
22. Wang CH, Wang CH, Hung PJ, Wei YH. Disruption of mitochondria-associated ER membranes impairs insulin sensitivity and thermogenic function of adipocytes. *Front Cell Dev Biol*. 2022;10:965523. doi:10.3389/fcell.2022.965523
23. Qiao D, Zhang Z, Zhang Y, et al. Regulation of endoplasmic reticulum stress-autophagy: a potential therapeutic target for ulcerative colitis. *Front Pharmacol*. 2021;12:697360. doi:10.3389/fphar.2021.697360
24. Hetz C, Zhang K, Kaufman RJ. Mechanisms, regulation and functions of the unfolded protein response. *Nat Rev Mol Cell Biol*. 2020;21 (8):421–438. doi:10.1038/s41580-020-0250-z
25. Zheng Z, Shang Y, Tao J, Zhang J, Sha B. Endoplasmic reticulum stress signaling pathways: activation and diseases. *Curr Protein Pept Sci*. 2019;20(9):935–943.DOI:10.2174/1389203720666190621103145.
26. Zhu Y, Xie M, Meng Z, et al. Knockdown of TM9SF4 boosts ER stress to trigger cell death of chemoresistant breast cancer cells. *Oncogene*. 2019;38(29):5778–5791. doi:10.1038/s41388-019-0846-y
27. Kong M, Han Y, Zhao Y, Zhang H. miR-512-3p overcomes resistance to cisplatin in retinoblastoma by promoting apoptosis induced by endoplasmic reticulum stress. *Med Sci Monit*. 2020;26:e923817. doi:10.12659/MSM.923817
28. Zhang Y, Yuan Y, Liang P, et al. Overexpression of a novel candidate oncogene KIF14 correlates with tumor progression and poor prognosis in prostate cancer. *Oncotarget*. 2017;8(28):45459–45469. doi:10.18632/oncotarget.17564
29. Meng F, Zhang Z. MicroRNA-152 specifically targets kinesin family member 14 to suppress the advancement of bladder cancer cells via PI3K/AKT pathway. *Biochem Biophys Res Commun*. 2024;692:149337. doi:10.1016/j.bbrc.2023.149337
30. Huang W, Wang J, Zhang D, et al. Inhibition of KIF14 suppresses tumor cell growth and promotes apoptosis in human glioblastoma. *Cell Physiol Biochem*. 2015;37(5):1659–70.DOI:10.1159/000438532.
31. Xu H, Zhao G, Zhang Y, et al. Long non-coding RNA PAXIP1-AS1 facilitates cell invasion and angiogenesis of glioma by recruiting transcription factor ETS1 to upregulate KIF14 expression. *J Exp Clin Cancer Res*. 2019;38(1):486. doi:10.1186/s13046-019-1474-7
32. Daisy Precilla S, Biswas I, Kuduvalli SS, Anitha TS. Crosstalk between PI3K/AKT/mTOR and WNT/β-Catenin signaling in GBM - Could combination therapy checkmate the collusion. *Cell Signal*. 2022;95:110350. doi:10.1016/j.cellsig.2022.110350
33. Mortazavi M, Moosavi F, Martini M, Giovannetti E, Firuzi O. Prospects of targeting PI3K/AKT/mTOR pathway in pancreatic cancer. *Crit Rev Oncol Hematol*. 2022;176:103749. doi:10.1016/j.critrevonc.2022.103749
34. Paskeh M, Ghadyani F, Hashemi M, et al. Biological impact and therapeutic perspective of targeting PI3K/Akt signaling in hepatocellular carcinoma: promises and challenges. *Pharmacol Res*. 2023;187:106553. doi:10.1016/j.phrs.2022.106553
35. Murugan AK. Special issue: PI3K/Akt signaling in human cancer. *Semin Cancer Biol*. 2019;59:1–2. doi:10.1016/j.semcancer.2019.10.022
36. Murugan AK. mTOR: role in cancer, metastasis and drug resistance. *Semin Cancer Biol*. 2019;59:92–111. doi:10.1016/j.semcancer.2019.07.003